RESEARCH ARTICLE

Dynamic behavior of detonation waves in millimeter-scale tubes: unraveling the influence of tube diameter, initial pressure, and mixture

Zhenhua Pan[1] · **Nan Jiang**[1] · **Jian Zhou**[1] · **Penggang Zhang**[1]

Abstract

This study investigates the flame propagation behaviors of three different mixtures ($C_2H_4 + 3O_2$, $C_3H_8 + 5O_2$, and $C_2H_2 + 2.5O_2 + 3.5Ar$) in millimeter-scale tubes, unraveling their distinct propagation characteristics at the flame front. The experiments consider variations in mixture, initial pressure, and tube diameter, revealing shared features among them. The results indicate that, for a stable mixture, the experimentally calculated velocity deficits closely align with the theoretical predictions. However, when dealing with an unstable mixture, the velocity deficit calculated using Fay's theory is found to be significantly overestimated. With decreasing tube diameter and initial pressure, the propagation of detonation waves exhibits periodic oscillations, such as galloping and stuttering. Additionally, the relationship between initial pressure and detonation cell width is explored, introducing the parameter (d/λ) to characterize detonation propagation capability. The experimental results demonstrate that for unstable mixtures, as the tube diameter decreases, the value of (d/λ) gradually increases, indicating that smaller tube diameters facilitate unstable detonation propagation. However, for stable mixtures, the value of (d/λ) exceeds the expected theoretical value, suggesting a higher initial pressure requirement compared to unstable mixtures for achieving detonation propagation.

1 Introduction

Compared to conventional deflagration-based systems, detonation-based propulsive systems offer higher thermodynamic efficiency (Powers et al. 2006) Consequently, in recent decades, numerous researchers have focused on applying controlled detonation waves in innovative propulsive system concepts, such as the pulse detonation engine (PDE) (Roy et al. 2004; Zhang et al. 2020a, b), rotating detonation engine (RDE) (Lu et al. 2014), and standing detonation engine (SDE) (Teng et al. 2022). This has led to the detonation phenomenon becoming a prominent research topic with significant theoretical and practical applications.

One of the critical technologies in detonation-based engines is the rapid initiation of detonation in the combustion chamber. Previous studies have demonstrated that using

small-diameter tubes as pre-detonators can effectively initiate detonation (Wolański 2013; Li et al. 2019; Jia et al. 2022). However, in confined spaces where the tube diameter is smaller than the characteristic length of the mixture, detonation waves cannot propagate due to substantial momentum and heat loss to the walls (Zhu et al. 2017; Pan et al. 2017; Zhang et al. 2019). The detonation velocity in such tubes is usually lower than the theoretical Chapman–Jouguet (C–J) value. This is attributed to the fact that the detonation velocity calculated by the C–J theory, which depends solely on the thermodynamic properties of the explosive mixture, remains unaffected by boundary conditions. When a detonation wave propagates in a channel with obstructions (Kellenberger et al. 2017; Rainsford et al. 2018), porous walls (Radulescu and Lee 2002; Mazaheri et al. 2015), a small tube (Wu et al. 2007, 2011), or a narrow channel (Ishii and Tsuboi 2002; Sow et al. 2017), momentum and heat losses occur (Sow et al. 2019). These losses to the wall reduce the detonation velocity from its theoretical C–J value. In millimeter-scale channels, the boundary layer (BL) can cause significant momentum and heat losses, resulting in a velocity deficit for the detonation wave. Ishii and Tsuboi (2002) experimentally investigated the detonation velocity deficit

✉ Penggang Zhang
zhangpg@ujs.edu.cn

1 School of Energy Resources and Power Engineering, Jiangsu University, Zhenjiang 212013, Jiangsu, People's Republic of China

in narrow gaps ranging from 0.8 to 3 mm. They observed that BL effects, such as wall friction and heat loss, lead to decreased pressure and temperature behind the shock wave (SW) front, resulting in a velocity deficit proportional to $h_g^{-0.8}$, where h_g represents the gap size. Specific analyzes of the velocity deficit due to wave-front curvature can be found in studies by Yao et al. (1995), Klein et al. (1995), and Radulescu and Lee (2002). Chinnayya et al. (2013) and Sow et al. (2017) noted that the wall dissipation effect becomes more pronounced as the tube diameter decreases. This effect suppresses transverse instability, leading to larger cell sizes and increased velocity deficits. Xiao et al. (2021) evaluated the impact of BL losses in narrow channels on the detonation velocity of an H_2–O_2–Ar mixture. They employed Mirels' theoretical model to simulate BL losses by incorporating the three-dimensional flow divergence effect caused by the BL displacement thickness (Mirels et al. 1956). The increase in the Mirels constant resulted in a corresponding decrease in detonation velocity. However, for unstable detonation characterized by an irregular cellular structure, the experimental detonation velocity deficit does not align with the value calculated using Fay's quasi-1D theory (Fay et al. 1959). This discrepancy arises because the propagation mechanism of unstable detonation is primarily governed by instability, which is less influenced by BL effects. Immediately after this, Xiao et al. (2023) demonstrated that small-scale cellular structures have a negligible impact on the macro-scale propagation mechanism of stable detonation. They successfully established a general correlation for characterizing the dynamics of hydrogen detonations in narrow channels and tubes.

Near the detonability limits, unstable detonation waves exhibit various propagation behaviors. Lee et al. (1995) and Haloua et al. (2000) observed a spectrum of unsteady propagation behaviors, including stuttering, galloping, low-speed deflagration (fast flame), and detonation extinction, using Doppler interferometry. These observations were made in relatively small-sized tubes. Manzhalei (1992) investigated the mechanism of the low-speed stage of galloping detonation propagation in capillaries and proposed that the BL effect plays a role in maintaining comparable velocities between the reaction front and the SW. However, this mechanism does not explain the occurrence of galloping detonation in large-diameter tubes where the BL is negligible. Gao et al. (2015) and Jackson et al. (2016) conducted detailed studies on galloping detonation in millimeter-scale spiral tubes. Notably, they observed the transition from the low-speed phase to overdriven detonation within a single cycle of galloping detonation. They attributed this behavior to the highly unstable nature and narrowness of the tube, which promote rapid amplification of small transverse perturbations. Smaller tube diameters result in higher frequencies of acoustic wave interactions and amplification at the tube wall.

Although the studies mentioned above have explored the quantitative relationship between velocity deficit and initial pressure or tube diameter, there is still a lack of comprehensive analysis considering the combined influence of both factors. Additionally, there exist significant differences in the mode of detonation propagation between millimeter-scale and larger-scale tubes (centimeter-scale). The BL effect can introduce velocity fluctuations, thereby influencing the determination of detonability limits. In this study, Fay's classical theory is employed to predict the detonation velocity deficit for different initial pressures and tube diameters. The predictions are then compared with experimental results to assess the reliability of Fay's theory for two types of mixtures: (i) an unstable mixture without argon dilution and (ii) a stable mixture with high dilution. Furthermore, by investigating various detonation behaviors near the detonability limits, we divide the range of initial pressures corresponding to the unstable detonation mode and establish a criterion for determining the detonability limit in millimeter-scale tubes.

2 Experimental details

Figure 1 depicts a schematic of the experimental setup. Transparent polycarbonate (PC) tubes with various inner diameters ($d = 0.5$ mm, 1.0 mm, 2.0 mm, and 4.0 mm) were utilized to investigate the characteristics of detonation propagation. The specific configuration of the experimental system is described in detail in our previously published paper (Pan et al. 2022). Three hydrocarbon fuels commonly found in petrochemical transport, namely C_2H_2, C_2H_4, and C_3H_8, were employed for the experiments. Two types of mixtures, referred to as stable and unstable mixtures, were chosen as the test gases. For a stable mixture (e.g., $C_2H_2 + 2.5O_2 + 3.5Ar$), the chemical reaction is insensitive to temperature variations, and the Zeldovich-von Neumann-Döring (ZND) model can be employed to characterize the detonation process (Zhang et al. 2014, 2018). Conversely, for an unstable mixture (e.g., $C_2H_4 + 3O_2$, $C_3H_8 + 5O_2$), a small temperature perturbation can lead to a significant change in the chemical reaction rate, resulting in rapid amplification of minor disturbances (Pan et al. 2019). Consequently, instabilities govern the detonation propagation, resulting in an irregular cellular structure.

Flame propagation was captured using a high-speed camera (Photron FASTCAM SA-Z). The local flame velocity was determined by calculating the ratio of the distance between the flame fronts in consecutive frames to the time interval between those frames. Details regarding the measurement method of local velocity and the evaluation of errors can be found in our previously published papers (Zhang et al. 2021; Pan et al. 2022). To ensure the accuracy and reliability of the results, experiments under the same
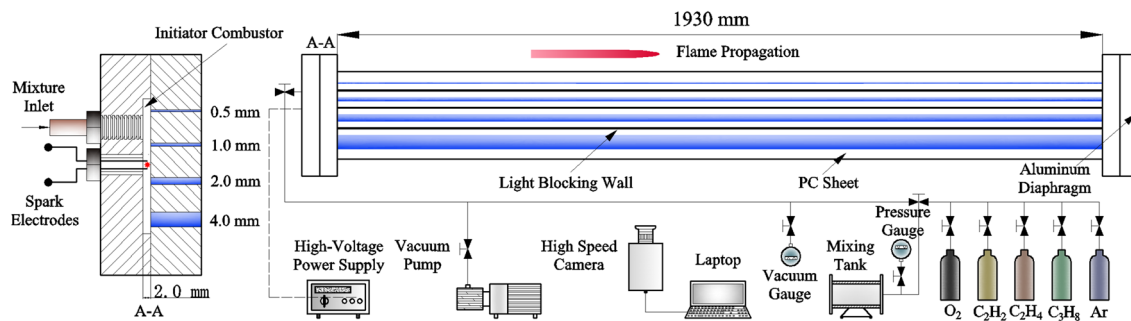
Fig. 1 Schematic of experimental apparatus

initial conditions were conducted and repeated at least three times.

3 Results and discussion

Figure 2 illustrates a representative sequence of high-speed images capturing the flame propagation in a 4-mm tube filled

Fig. 2 High-speed image sequences capturing the flames demonstrating Deflagration-to-Detonation Transition (DDT) and steady detonation propagation for the $C_2H_4 + 3O_2$ mixture at an initial pressure of 85 kPa. The interval between consecutive tick marks on the right-hand edge corresponds to 83.33 μs, equivalent to 10 frames. The image sequences depict flames in tubes with different diameters: **a** 4 mm, **b** 2 mm, **c** 1 mm, and **d** 0.5 mm
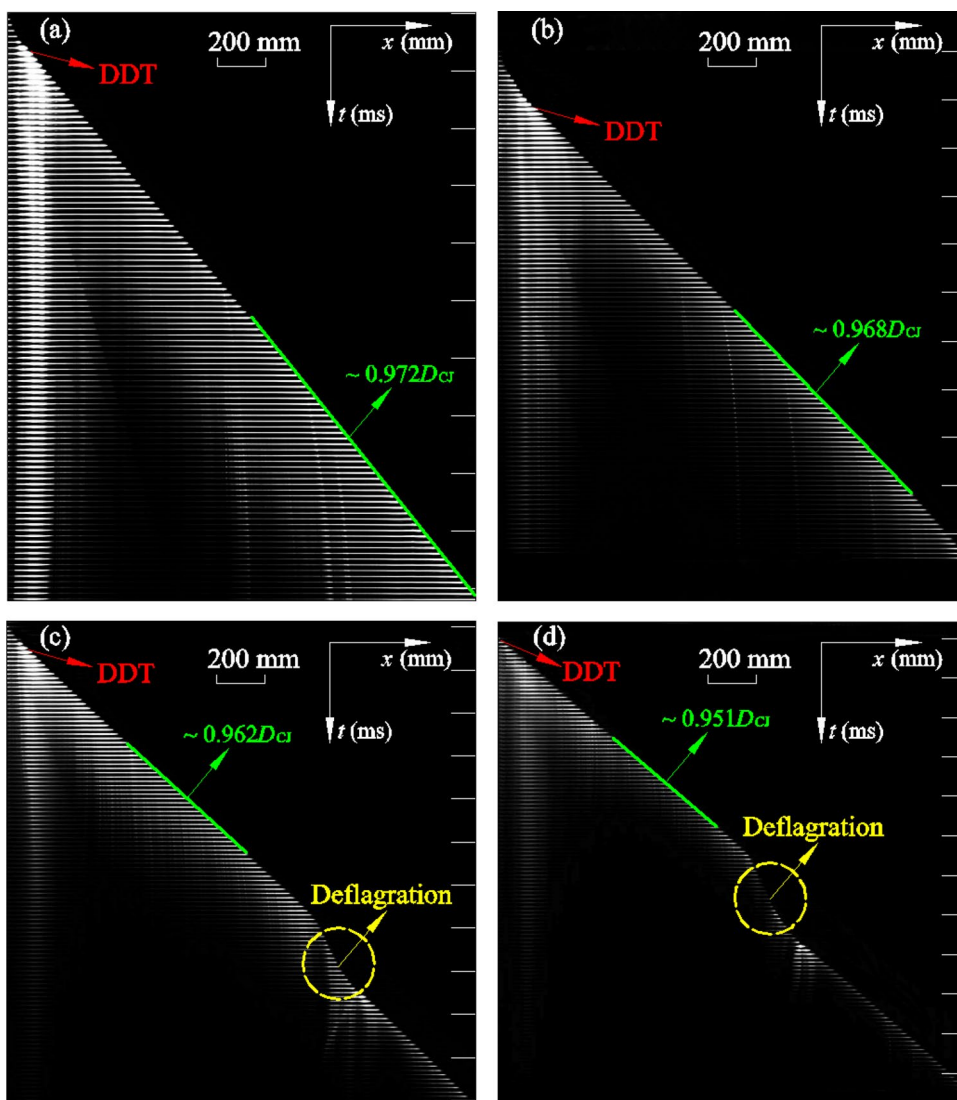
with $C_2H_4 + 3O_2$ at an initial pressure of 85 kPa. The experiments were conducted using a high-speed camera to capture the chemical autofluorescence of the flame. The frame rate for each experiment was set to 120,000 frames per second, resulting in a time interval of 8.333 microseconds between two adjacent frames. The local velocity of the flame (D) was calculated as the ratio of the distance between the flame front in adjacent frames (Δx) to the time interval between adjacent frames (Δt), expressed as $D = \Delta x / \Delta t$. Upon observation of the images, it was evident that the flame propagation velocities closely matched the theoretical Chapman–Jouguet (C–J) velocity following the deflagration to detonation transition (DDT) process. The interval between consecutive tick marks on the right edge of the image represents 83.33 μs (equivalent to 10 frames). The trajectory lines depicting the evolution of the flame tip over time exhibit both nonlinear and linear variations, corresponding to the deflagration phase (depicted by the yellow cycle) and the steady detonation phase (indicated by the solid green line), respectively. The instantaneous onset of detonation is marked by a boundary (indicated by the red arrow), clearly distinguishing the deflagration from the detonation phase. It is important to note that the chemiluminescence observed in the flame represents the intensity of the chemical reaction, providing an indication of the flame burning rate.

Figure 3 illustrates the evolution of flame propagation velocity in tubes of four different inner diameters, corresponding to the high-speed image sequences of flames shown in Fig. 2. The specific local flame velocity was calculated through the following steps: First, the excess area of the image, where the flame was not captured by the high-speed camera, was cropped. The cropped image was 978×244 pixels, corresponding to a visualization length of 1930 mm. Each pixel point in the image represented a length of 1.973 mm along the tube. To enhance the quality of the cropped image for clearer identification of the flame front, the pixels of the cropped image were increased to 5000 in the flame propagation direction. Consequently, each pixel point represented a physical length of 0.386 mm. The local flame propagation velocity was then calculated using the formula $D = 386(x_{i+1} - x_i)/8.333$, where x_i and x_{i+1} represent the positions of adjacent flame fronts, and 8.333 microseconds represented the time interval between two adjacent frames. It is essential to note that when identifying the flame tip, variations in chemical reaction luminescence intensity led to an error of ± 1 pixel. Considering the spatial resolution of 0.386 mm per pixel, a misinterpretation of one pixel
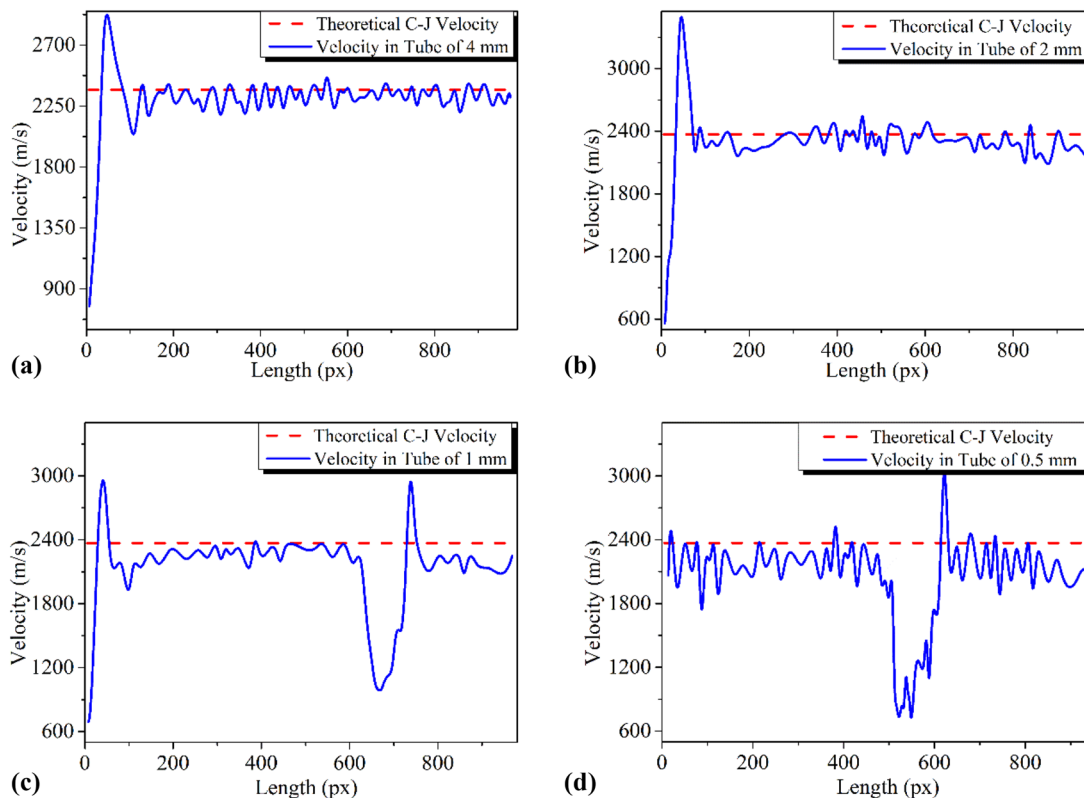
Fig. 3 Flame velocity distribution along the four tubes for $C_2H_4 + 3O_2$ at an initial pressure of 85 kPa: $d =$ (**a**) 4 mm, (**b**) 2 mm, (**c**) 1 mm, and (**d**) 0.5 mm

introduced an uncertainty of approximately 46 m/s in the velocity data presented. The continuous curve representing the velocity distribution was obtained by interpolating the discrete data. It was evident from the analysis that flames exhibited self-acceleration, nearly reaching the theoretical Chapman–Jouguet (C–J) detonation velocity (DCJ) in all four tube sizes, indicating presence of detonation waves. Importantly, when the flame propagation velocity approached the theoretical C–J value, the maximum relative error did not exceed 3%. Well within the detonability limits, where the tube diameter significantly exceeds the critical tube diameter, the propagation velocity of the detonation wave remains relatively stable around the theoretical C–J value with minor fluctuations (as observed in Fig. 3a and b). Similar fluctuations in nature and amplitude were previously observed in time-resolved measurements conducted by Lee et al. (1995) and Haloua et al. (2000) using microwave interferometry. These researchers suggested that random fluctuations can effectively cancel each other out when averaging the velocities, thereby not significantly affecting the overall average velocity of the detonation wave. In our measurements, the calculated average flame velocity, after the velocity jump, approximates $0.97D_{CJ}$. However, near the detonability limits, the flame velocity exhibits notable oscillatory characteristics (as seen in Fig. 3c and d). The flame velocity experiences a minimum drop to approximately $0.5D_{CJ}$, followed by a subsequent overdrive detonation that raises the velocity above D_{CJ}. This observed phenomenon bears resemblance to that of a galloping detonation (Gao et al. 2015). In our study, due to limitations in tube length, only one cycle of velocity decay was observed. Notwithstanding the brief period of low-velocity propagation experienced by the flame, its velocity remains around $0.9D_{CJ}$.

For steady detonation propagation, the local flame velocity can be considered as the detonation velocity since the flame front closely follows the leading SW. In Fig. 4, the local flame front velocities at different locations are shown for the $C_2H_4 + 3O_2$ mixture in the 2-mm and 4-mm tubes at initial pressures of 25 kPa and 55 kPa, respectively. The purpose of this analysis is to investigate the relationship between the measured average detonation velocity (D_{ave}) and the initial pressure (p_0) or tube diameter (d). From Fig. 4, it is evident that the detonation propagates steadily to the end of the tube under each specific condition after the DDT process. Although there are slight fluctuations in the local velocities, these fluctuations are generally within 5%, indicating that the detonation propagation behaviors can be considered as steady. To calculate D_{ave} accurately, it is necessary to exclude the DDT stage and subsequent adjustment to avoid distorting the average velocity. D_{ave} is determined by calculating the ratio of the global propagation distance to the arrival time. The results demonstrate that, with a fixed tube diameter,
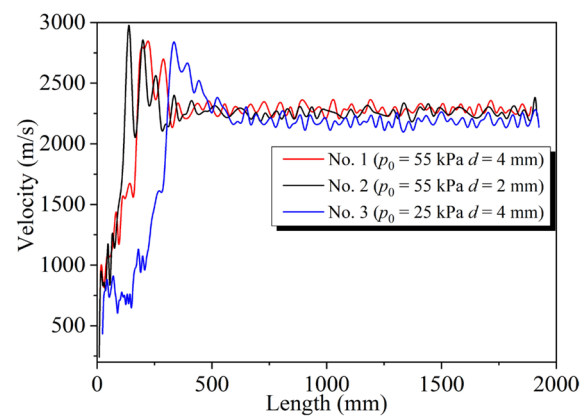
Fig. 4 Steady propagation detonation for various initial pressures and tube diameters

a lower initial pressure leads to a smaller value of D_{ave} due to the decreased detonability sensitivity. On the other hand, with a fixed initial pressure, D_{ave} decreases as the tube diameter decreases. To further analyze the data, D_{ave} can be normalized with the D_{CJ}, yielding the velocity deficit (ΔD_m)

$$\Delta D_m = \frac{D_{CJ} - D_{ave}}{D_{CJ}}, \tag{3.1}$$

By examining Fig. 4, we can observe the velocity deficits for different cases. In particular, for Case No. 1 with an initial pressure of 55 kPa and tube diameter of 4 mm, the velocity deficit is 2.4% of D_{CJ}. In Case No. 2, which also has an initial pressure of 55 kPa but a tube diameter of 2 mm, the velocity deficit is 3.8% of D_{CJ}. Lastly, in Case No. 3 with an initial pressure of 25 kPa and tube diameter of 4 mm, the velocity deficit is 5.2% of D_{CJ}. The results suggest that lower initial pressures and smaller tube diameters result in larger deviations from the theoretical C–J velocity.

For detonation propagation near the detonability limits, the average velocity is close to the theoretical C–J value. However, it is important to note that these detonations also exhibit a low-velocity propagation phase that is not meaningful for evaluating velocity loss. The detonation velocity deficit can be attributed to BL effects that originate from the tube walls, particularly in millimeter-scale tubes. Fay's theory (1959) provides a framework for understanding and quantifying the detonation velocity deficit. It is based on the conservation equations of quasi-1D flow, which consider the effects of BL on the detonation wave. By applying Fay's theory, we can derive the detonation velocity deficit and assess its impact on the overall detonation propagation. This analysis helps us understand the influence of

BL and its contribution to the observed velocity deviations from the theoretical C–J velocity. Therefore, ΔD_m can also be expressed as

$$\Delta D_m = \frac{D_{CJ} - D_{ave}}{D_{CJ}} = 1 - \left[\frac{(1-v)^2}{(1-v)^2 + \gamma^2(2v - v^2)}\right]^{1/2}, \quad (3.2)$$

where γ is the ratio of specific heats under the C–J condition, and v can be expressed as

$$v = \frac{\xi}{(1+\gamma)(1+\xi)}, \quad (3.3)$$

where ξ is the fractional increase in area of any stream tube compared with its area at the SW, which is given by following equations

$$\xi = \frac{A}{A_0} - 1 = \frac{\pi(R + \delta^*)^2}{\pi R^2} - 1 \approx \frac{2\delta^*}{R} = \frac{4\delta^*}{d}, \quad (3.4)$$

$$\delta^* = 0.22 x^{0.8}\left(\frac{\mu_e}{\rho_0 V}\right)^{0.2}, \quad (3.5)$$

Figure 5 shows the relationship between the detonation velocity deficit and the tube diameter and initial pressure for the three mixtures. The solid line is the curve fitted to the experimental data, and the dashed line denotes the values calculated by Fay's theory. The experimental velocity deficit can be expressed as.

$$\Delta D_m = A \cdot d^a p_0^b, \quad (3.6)$$

where the values of the coefficient A and exponents a and b are given in Table 1. As Fig. 4 shows, the velocity deficit is inversely proportional to the tube diameter or initial pressure.

Table 1 Detonation velocity deficit as function of initial pressure and tube diameter as given by $\Delta D = A \cdot d^a p_0^b$

Mixture	A	a	b
$C_2H_4 + 3O_2$	4.87	-0.69	-1.04
$C_3H_8 + 5O_2$	5.09	-0.76	-1.06
$C_2H_2 + 2.5O_2 + 3.5Ar$	5.37	-0.71	-1.01
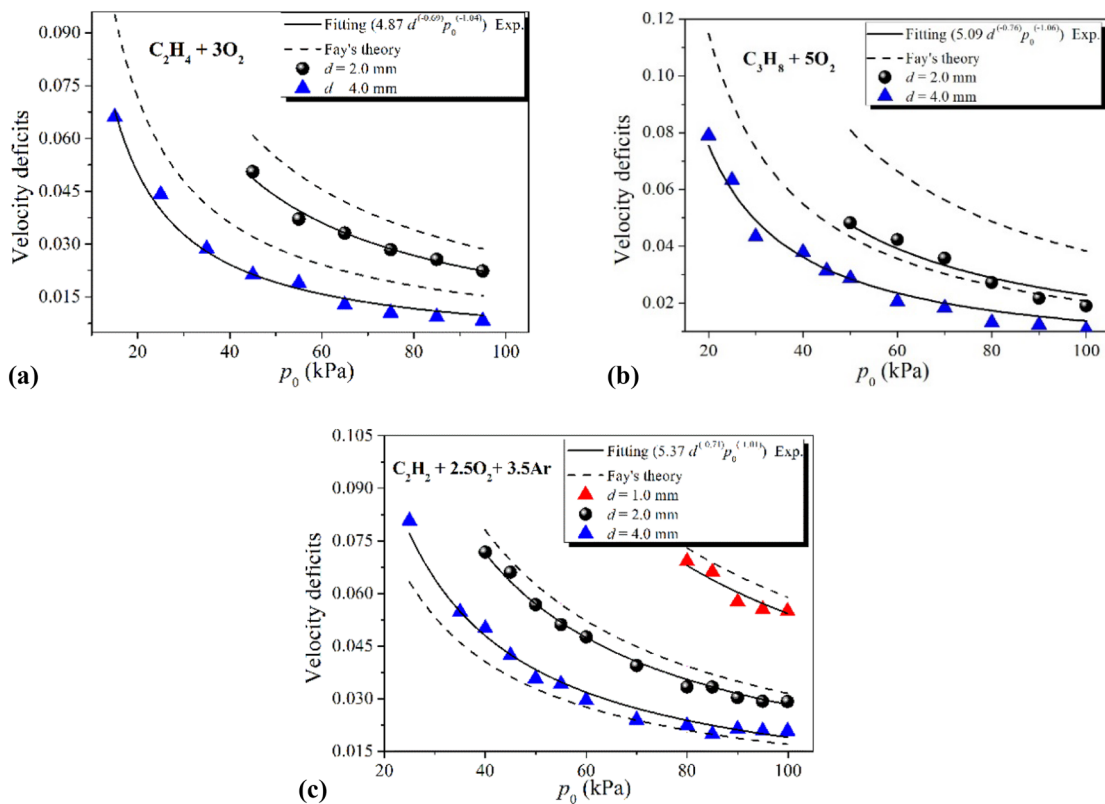
Fig. 5 Relationships between detonation velocity deficit and initial pressure for different tube diameters: (**a**) $C_2H_4 + 3O_2$; (**b**) $C_3H_8 + 5O_2$; (**c**) $C_2H_2 + 2.5O_2 + 3.5Ar$
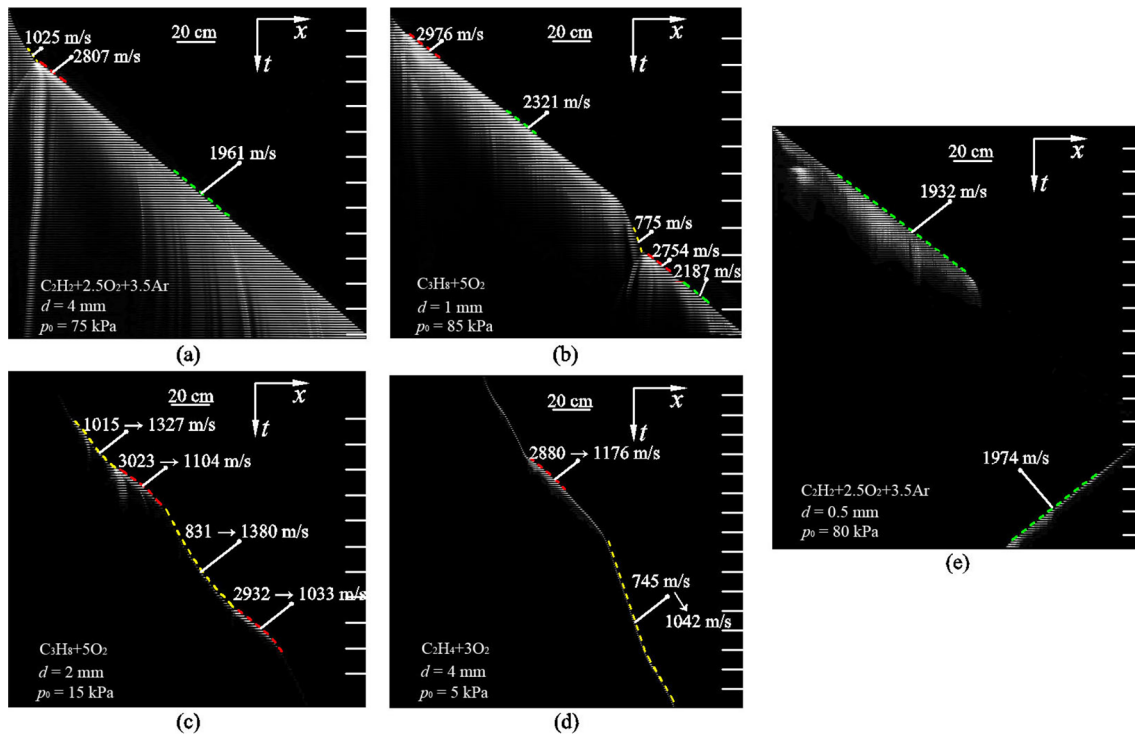
Fig. 6 High-speed image sequences of flames showing DDT and steady detonation propagation. The interval between consecutive tick marks on the right-hand edge represents 83.33 μs (10 frames): (**a**) $C_2H_2+2.5O_2+3.5Ar$ mixture at 75-kPa initial pressure in 4-mm tube; (**b**) $C_3H_8+5O_2$ mixture at 85-kPa initial pressure in 1-mm tube; (**c**) $C_3H_8+5O_2$ mixture at 15-kPa initial pressure in 2-mm tube; (**d**) $C_2H_4+3O_2$ mixture at 5-kPa initial pressure in 4-mm tube; (**e**) $C_2H_2+2.5O_2+3.5Ar$ mixture at 80-kPa initial pressure in 0.5-mm tube

In Fig. 5a and b, it is observed that the theoretically predicted detonation velocity deficit deviates from the experimental values by approximately 20%, indicating that the theoretically calculated values are overestimated. On the other hand, in Fig. 5c, the deviation is within 6%, suggesting that Fay's quasi-1D model can effectively predict velocity deficits in millimeter-scale tubes. The difference between Fig. 5a, b, and c can be attributed to the distinct propagation mechanisms of the detonation waves in the two types of mixtures.

For unstable detonation ($C_2H_4+3O_2$ and $C_3H_8+5O_2$), the propagation mechanism is primarily influenced by the instability of the detonation wave. When the negative displacement effect of the BL becomes significant, the unstable detonation wave generates new transverse waves to compensate for this effect, thereby maintaining overall propagation near the theoretical C–J velocity. These transverse waves can originate from the amplification of small perturbations or explosive bubbles formed by unreacted gas pockets, as suggested by Oran et al. (1982) and Radulescu and Lee (2002). Consequently, unstable detonation is less sensitive to changes in boundary conditions. In contrast, for stable detonation ($C_2H_2+2.5O_2+3.5Ar$), the intensity of transverse waves is relatively weak, and they can be considered as acoustic oscillations in the product zone. Thus, the number of transverse waves only reflects the intensity of detonation and does not control the propagation itself. When the effect of negative displacement becomes significant, the strength of the stable detonation is prone to weakening. The propagation mechanism in this case is predominantly governed by the adiabatic compression of the leading SW based on the ZND model. Since Fay's quasi-1D theory is derived from the ZND model, the theoretically calculated values align well with the observed stable detonation velocity deficits. Overall, the different behaviors observed in Fig. 5a, b, and c can be attributed to the distinct mechanisms governing the propagation of unstable and stable detonation waves, with Fay's quasi-1D theory proving to be effective in predicting the velocity deficits in millimeter-scale tubes, particularly for stable detonation scenarios.

The study conducted in millimeter-scale tubes with the three different mixtures ($C_2H_4+3O_2$, $C_3H_8+5O_2$, and $C_2H_2+2.5O_2+3.5Ar$) revealed diverse propagation behaviors of the flame front, which were observed by decreasing the initial pressure or the tube diameter. It is worth noting that despite the variations in mixtures, initial pressure, and tube diameters, there were certain common characteristics observed in the different cases.

Figure 6 shows five typical high-speed image sequences capturing different flame propagation behaviors. In Fig. 6a, a notable change in the slope of the flame-front trajectory is observed immediately after the DDT process. This behavior occurs well within the detonability limits of a 4-mm tube with a $C_2H_2 + 2.5O_2 + 3.5Ar$ mixture at an initial pressure of 75 kPa, where the detonation wave propagates steadily at a constant velocity. The slope of the trajectory determines the average detonation velocity, which measures approximately 1961 m/s, very close to the theoretical C–J value of 2006 m/s. It is worth noting that the C–J theory does not consider the influence of boundary conditions on detonation wave propagation, which explains the slight deviation between the experimental value and the theoretical C–J value. This regime represents the stage of steady detonation propagation. As the detonation sensitivity decreases or the inner tube diameter decreases, the behavior of the detonation wave exhibits oscillatory characteristics in terms of velocity and strength. Despite these fluctuations, the detonation wave retains its unique characteristics. In the behavior of stuttering detonation propagation, as depicted in Fig. 6b, the flame evolution is observed in a typical scenario near detonability limits. Specifically, this image sequence illustrates the behavior of the flame in a 1-mm tube filled with the $C_3H_8 + 5O_2$ mixture at an initial pressure of 85 kPa. Initially, the flame propagates rapidly at a velocity of 2321 m/s along the tube. However, at a distance of 1252 mm from the ignition spot, a sudden deceleration occurs, referred to as the "tumble down" phenomenon in the high-speed image sequence. This random velocity decay, also observed by Lee et al. (1995) and Zhang et al. (2016) in their studies on stuttering detonation, presents an intriguing propagation mechanism that is not yet fully understood. Following this hesitation, the flame re-accelerates and eventually propagates at a velocity near the theoretical C–J value. However, the average propagation velocity of the stuttering detonation wave is approximately 93% of the theoretical C–J value, further attenuated compared to the steadily propagating detonation wave. This attenuation highlights the unique characteristics of the stuttering detonation behavior and the impact of near detonability limits on the propagation behavior of the flame front.

The $CH_4 + 2O_2$ mixture serves as an example to illustrate the characteristics of the third detonation propagation behavior. The experiment is conducted in a 2-mm tube at an initial pressure of 15 kPa. From Fig. 6c, it is evident that the flame propagation velocity exhibits periodic oscillations (the four regions represented by arrows), which correspond to the flickering of flame brightness. Each propagation cycle consists of acceleration, detonation initiation, attenuation, and detonation extinction. In this particular experiment, the high-speed camera captures one complete cycle of propagation. The ratio of wavelength to tube diameter within the

cycle is approximately 300, consistent with the findings of galloping detonation observed by Gao et al. (2015) and Jackson et al. (2016). It is important to note that galloping detonation is a self-sustaining phenomenon with an intrinsic frequency. During the low-velocity phase, the galloping detonation mode propagates in a deflagration-like manner, yet the average velocity remains around 90% of the theoretical C–J value. This implies that galloping detonation can be considered as a plausible final detonation propagation mode near the detonability limits.

Beyond the limit conditions, the detonation wave ceases to exist within the tube, as depicted in Fig. 6d. Although the flame undergoes acceleration, indicated by a sudden and significant increase in brightness around 790 mm (2880 m/s) from the ignition end, successful initiation of detonation is hindered due to excessive heat loss of the burned gas to the tube walls. Subsequently, the flame gradually decelerates to the velocity of 745 m/s and eventually propagates toward the end of the tube at approximately half the theoretical C–J velocity. This behavior is reminiscent of the low-velocity detonation observed by Manzhalei (1992) in capillary tubes. Manzhalei found that the flame propagated at a speed similar to that of the leading SW, with a separation distance between them ranging from four to six times the tube diameter (assuming a laminar boundary layer). Lee (2008) referred to this phenomenon as high-speed deflagration, which is supersonic relative to the unburned gas ahead of the SW. Consequently, distinguishing whether this mode represents deflagration or detonation becomes challenging. Speculatively, this flame propagation mode can be attributed to the interplay between the net heat release and the negative displacement of the BL. In Fig. 6e, the flame is ultimately extinguished. Within the 0.5-mm tube, the detonation wave initially propagates at 1932 m/s but experiences a sudden failure at approximately 1200 mm from the ignition end. Subsequently, back propagation of the flame is observed at the exit end of the tube, with an average speed of 1974 m/s. It is possible that the reflected shock wave at the closed end ignites the compressed unburned gas left by the previous shock wave, leading to the initiation of detonation, which then propagates toward the ignition end of the tube.

The paragraph describes the maps of flame propagation behaviors in millimeter-scale tubes for three types of mixtures, presented in Fig. 7. These maps illustrate three distinct regions based on the observed behaviors: (I) detonation failure, (II) unsteady detonation propagation, and (III) steady detonation propagation. The range of initial pressure for detonation propagation near the detonability limits, such as galloping and stuttering detonation waves, becomes narrower as the tube diameter increases for unstable mixtures. This means that smaller diameter tubes more readily promote and sustain cyclic fluctuations in detonation. According to Fay's theory, the BL can influence the flow upstream of the C–J
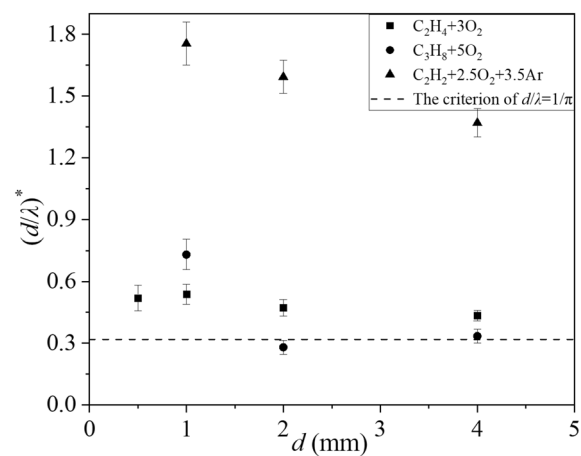
Fig. 7 Maps of flame propagation behaviors
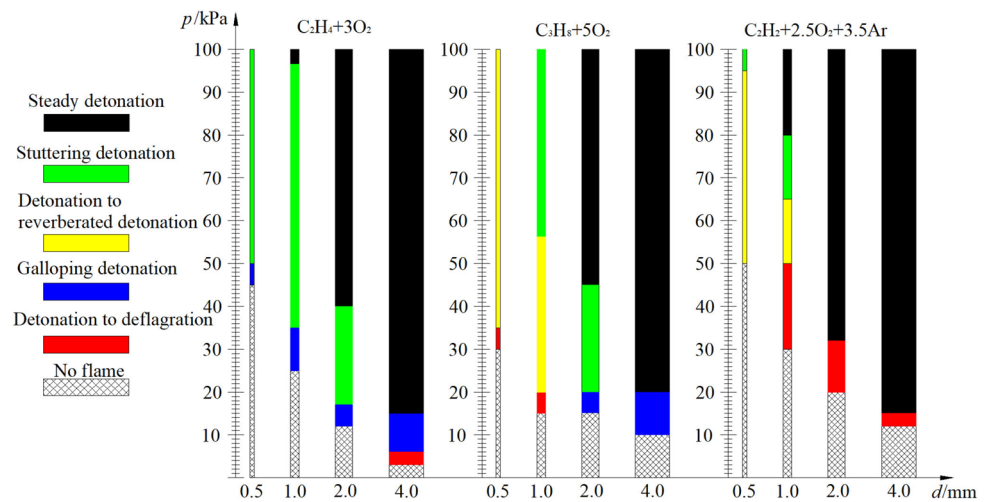
Table 2 Width of cellular structure correlations as function of the initial pressure given by $\lambda[mm] = C \cdot (p_0[kPa])^n$ for mixtures

Mixture	C	n
$C_2H_4 + 3O_2$	68.75	-1.1219
$C_3H_8 + 5O_2$	233.32	-1.2713
$C_2H_2 + 2.5O_2 + 3.5Ar$	59.76	-1.1146

Fig. 8 The detonability limit in the different tubes for three types of mixtures

plane, as the flow is subsonic relative to coordinates fixed in the SW. The negative displacement thickness caused by the BL results in leading shock curvature and even detonation failure (Fay 1959). This effect of the BL becomes increasingly significant with decreasing tube diameter. Additionally, transverse perturbations can grow rapidly during local failure of detonation propagation and can simulate an overdriven detonation if there is a high frequency of transverse perturbation interactions and reflections from the tube walls. Smaller tube diameters facilitate faster amplification of transverse waves. Therefore, for unstable mixtures, smaller tube diameters make unsteady detonation waves more likely to occur and widen the range of initial pressure. In contrast, for stable mixtures, detonation follows the ZND model, and the instability is less significant. This leads to the observation that detonation propagation, characterized by violent velocity fluctuations, is less likely to occur.

According to Fig. 7, the propagation of detonation waves is influenced by the diameter of the tube and the initial pressure. The detonability limit represents the condition beyond which steady self-sustained propagation of a detonation wave is not possible. In this study, the initial pressure is used to determine the width of the detonation cell, denoted as λ. The parameter d/λ, where d is the tube diameter, is introduced as a sensitive parameter to characterize the capability of detonation propagation. The relationship between the initial pressure and detonation cell width can be determined

by applying the least squares method to data extracted from the Caltech detonation database for the test mixtures. Table 2 shows the results of this analysis. In Lee's previous work on centimeter-scale tubes (Lee 1984), the detonability limit was considered to be $(d/\lambda)^* = 1/\pi$. Gao et al. (2014a, b) and Zhang et al. (2020a, b) further confirmed that this criterion is applicable across a range of tube diameters and should indeed be valid for microscale tubes. This means that detonation waves usually propagate in tubes with a diameter of at least one-third of λ, following the λ/π rule. Figure 8 presents the detonability limits for the three mixtures in different tube diameters. For unstable mixtures, $(d/\lambda)^*$ is approximately $1/\pi$ for tube diameters of 2 and 4 mm. Notably, as the tube diameter decreases, $(d/\lambda)^*$ gradually increases, indicating that smaller tube diameters require more sensitive mixtures for successful detonation propagation. Considering the uncertainty in measuring the detonation cell width, the range of detonability limits corresponds to $0.298 < (d/\lambda)^* < 0.746$.

In the case of stable mixtures, $(d/\lambda)^*$ is much greater than $1/\pi$, ranging from 1.3 to 1.8. This suggests that a higher initial pressure is needed to reach the detonability limit in stable mixtures compared to unstable mixtures for a given tube diameter. Consequently, the λ/π rule is not applicable for predicting the detonability limit of stable mixtures in millimeter-scale tubes.

4 Conclusions

In the context of detonation, unlike deflagration where the flame speed is subsonic with respect to the unburned mixture, the detonation wave is supersonic with respect to the unburned mixture ahead. However, there exists a subsonic region between the leading SW and the C–J surface, within which the BL develops. The energy released by chemical reactions within the BL does not fully support the propagation of the detonation wave, resulting in a velocity deficit compared to the theoretical C–J velocity. Based on Fay's quasi-1D theory, a quantitative relationship can be established between the velocity deficit (ΔD_m) and the initial pressure (p_0) as well as the tube diameter (d), expressed as $\Delta D_m = A d^a p_0^b$. This equation captures the influence of initial pressure and tube diameter on the velocity deficit of the detonation wave. For stable detonations, the calculated values obtained from this equation align well with experimental observations. However, for unstable detonations, the presence of instability regeneration mechanisms ensures that the detonation wave is not globally extinguished. This leads to the phenomenon of detonation instability, where the detonation wave exhibits fluctuations and oscillations in its propagation. In such cases, the velocity deficit predicted theoretically tends to be overestimated significantly compared to experimental measurements.

The experimental results obtained in millimeter-scale tubes reveal various flame propagation behaviors. When operating near the detonability limits, the velocities of detonation waves display longitudinal oscillations, primarily observed in unstable mixtures. It is found that as the tube diameter decreases, the range of initial pressure corresponding to the unstable propagation regime widens. On the other hand, for stable mixtures, the impact of instability on detonation wave propagation is minimal. Consequently, the periodic velocity oscillations observed in unstable mixtures, such as galloping, are not observed. The boundary layer plays a significant role in the propagation of detonation waves, and its influence on the detonability limit is substantial. Therefore, relying solely on the criterion of $\lambda = \pi d$ to predict the detonability limit is unreliable in millimeter-scale tubes. The complex interplay between the boundary layer and detonation wave dynamics necessitates a more comprehensive understanding of the underlying mechanisms to accurately predict detonation behavior in such confined systems.

The findings suggest that different propagation regimes, such as steady detonation, stuttering detonation, and galloping detonation, emerge as the flame approaches the limits of detonability, showcasing distinct behaviors and contributing to a deeper understanding of detonation wave dynamics. However, the complexity of instability dynamics makes it challenging to precisely predict the behavior of unstable detonation waves based solely on theoretical calculations. While there were variations in the specific behaviors and characteristics observed in the different mixtures, initial pressures, and tube diameters, the overall study highlighted the importance of considering the stability of the detonation wave and the impact of the boundary layer in understanding the propagation behaviors of the flame front in millimeter-scale tubes. The findings contribute to our knowledge of detonation wave dynamics and provide insights for further research and applications in this field.

Declarations

Conflict of interest The authors have no competing interests to declare that are relevant to the content of this article.

Informed consent All the co-authors have been informed and all gave explicit consent to submit this article. They also obtained consent from the responsible authorities at the institute/organization where the work has been carried out.

Ethical approval Not applicable.

References

Chinnayya A, Hadjadj A, Ngomo D (2013) Computational study of detonation wave propagation in narrow channels. Phys Fluids 25(3):036101

Fay J (1959) Two-dimensional gaseous detonations: velocity deficit. Phys Fluids 2(3):283–290

Gao Y, Lee JHS, Ng HD (2014a) Velocity fluctuation near the detonation limits. Combust Flame 161(11):2982–2990

Gao Y, Ng HD, Lee JHS (2014b) Minimum tube diameters for steady propgation of gaseous detonations. Shock Waves 24:447–454

Gao Y, Ng HD, Lee JHS (2015) Experimental characterization of galloping detonations in unstable mixtures. Combust Flame 162(6):2405–2413

Haloua F, Brouillette M, Lienhart V, Dupre G (2000) Characteristics of unstable detonations near extinction limits. Combust Flame 122(4):422–438

Ishii K, Tsuboi T (2002) A study on velocity deficits of detonation waves in narrow. Proc Combust Inst 29:2789–2794

Jackson S, Lee BJ, Shepherd JE (2016) Detonation mode and frequency analysis under high loss conditions for stoichiometric propane-oxygen. Combust Flame 167(5):24–38

Jia X, Zhao N, Maxwell B, Chen X, Zheng H (2022) Numerical research on effect of sudden cross-section expansion on detonation initiation. J Therm Sci 31(5):1575–1590

Kellengerger M, Ciccarelli G (2017) Simultaneous schlieren photography and soot foil in the study of detonation phenomena. Exp Fluids 58:138

Klein R, Krok JC, Shepherd JE (1995) Curved quasi-steady detonations: Asymptotic analysis and detailed chemical kinetics. GALCIT report FM 95−04, California Institute of Technology

Lee JHS (1984) Dynamic parameters of gaseous detonations. Ann Rev Fluid Mech 16:311–336

Lee JHS (2008) The detonation phenomenon. Cambridge University Press

Lee JJ, Dupre G, Knystautas R, Lee JH (1995) Doppler interferometry study of unstable detonations. Shock Waves 5(10):175–181

Li G, Ukai T, Kontis K (2019) Characterization of a novel open-ended shock tube facility based on detonation transmission tubing. Aerosp Sci Technol 94:105388

Lu FK, Braun EM (2014) Rotating detonation wave propulsion: experimental chal-lenges, modeling, and engine concepts. J Propuls Power 30:1125–1142

Manzhalei VI (1992) Detonation regimes of gases in capillaries. Combust Explos Shock Waves 28(5):296–302

Mazaheri K, Mahmoudi Y, Sabzpooshani M, Radulescu MI (2015) Experimental and numerical investigation of propagation mechanism of gaseous detonation in channels with porous walls. Combust Flame 162(6):2638–2689

Mirels H (1956) Boundary layer behind shock or thin expansion wave moving into stationary. Fluid NACA TN 3712

Oran ES, Young TR, Boris JP, Picone JM, Edwards DH (1982) A study of detonation structure: the formation of unreacted gas pockets. Proc Combust Inst 19(1):573–582

Pan ZH, Chen KP, Pan JF, Zhang PG, Zhu YJ, Qi J (2017) An experimental study of the propagation characteristics for a detonation wave of ethylene/oxygen in narrow gaps. Exp Therm Fluid Sci 88(11):354–360

Pan ZH, Chen KP, Qi J, Zhang PG, Zhu YJ, Pan JF, Gui MY (2019) The propagation characteristics of curved detonation wave: experiments in helical channels. Proc Combust Inst 37:3585–3592

Pan ZH, Zhang ZH, Zhang PG (2022) Effects of a significant boundary layer on the flame acceleration and transition to detonation in millimeter-scale tubes. Aerosp Sci Technol 126:107533

Powers JM, Frolov SM (2006) Introduction: perspectives on detonation-based propulsion. J Propuls Power 22(6):1153–1154

Radulescu MI, Lee JHS (2002) The failure mechanism of gaseous detonations: experiments in porous wall tubes. Combust Flame 131(1–2):29–46

Rainsford G, Aulakh DJS, Ciccarelli G (2018) Visualization of detonation ropagation in a round tube equipped with repeating orifice plates. Combust Flame 198:205–221

Roy GD, Frolov SM, Borisov AA, Netzer DW (2004) Pulse detonation propulsion: challenges, current status, and future perspective. Prog Energy Combust Sci 30:545–672

Sow A, Semenko RE, Kasimov AR (2017) On a stabilization mechanism for low-velocity detonations. J Fluid Mech 816(3):539–553

Sow A, Chinnayya A, Hadjadj A (2019) On the viscous boundary layer of weakly unstable detonations in narrow channels. Comput Fluids 179(1):449–458

Teng H, Ng HD, Li K, Luo C, Jiang Z (2022) Evolution of cellular structures on oblique detonation wurfaces. Combust Flame 162:342–348

Wolański P (2013) Detonative propulsion. Proc Combust Inst 34:125–158

Wu MH, Burke MP, Son SF, Yetter RA (2007) Flame acceleration and the transition to detonation of stoichiometric ethylene/oxygen in microscale tubes. Proc Combust Inst 31(2):2429–2436

Wu MH, Wang CY (2011) Reaction propagation modes in millimeter-scale tubes for ethylene/oxygen mixtures. Proc Combust Inst 33(2):2287–2293

Xiao Q, Sow A, Maxwell B, Radulescu MI (2021) Effect of boundary layer losses on 2D detonation cellular structures. Proc Combust Inst 38(3):3641–3649

Xiao Q, Weng CS (2023) Unified dynamics of hydrogen-oxygen-diluent detonations in narrow confinements. Fuel 334:126661

Yao J, Stewart DS (1995) On the normal detonation shock velocity-curvature relationship for materials with large activation energy. Combust Flame 100(4):519–528

Zhang B, Mehrjoo N, Ng HD, Lee JHS, Bai CH (2014) On the dynamic detonation parameters in acetylene–oxygen mixtures with varying amount of argon dilution. Combust Flame 161(5):1390–1397

Zhang B, Wang C, Shen XB, Yan L, Yan BJ, Xia Y (2016) Velocity fluctuation analysis near detonation propagation limits for stoichiometric methane-hydrogen-oxygen mixture. Int J Hydrog Energy 41(39):17750–17759

Zhang B, Liu H, Wang CH (2018) Detonation propagation limits in highly argon diluted acetylene-oxygen mixtures in channels. Exp Therm Fluid Sci 90:125–131

Zhang B, Liu H (2019) Theoretical prediction model and experimental investigation of detonation limits in combustible gaseous mixtures. Fuel 258:116132

Zhang B, Liu H, Yan BJ, Ng HD (2020a) Experimental study of detonation limits in methane-oxygen mixtures: determining tube scale and initial pressure effects. Fuel 259:116220

Zhang PG, Pan ZH, Zhu YJ, Wang Q, He ZX (2021) Experimental study on the deflagration-to-detonation transition distance in millimeter-scale smooth tubes. AIAA J 59(8):3144–3151

Zhang Q, Qiao X, Fan W, Wang K, Tan F, Wang J (2020b) Study on operation and propulsion features of a pulse detonation rocket engine with secondary oxidizer injection. Appl Therm Eng 180:115661

Zhu YJ, Pan ZH, Zhang PG, Pan JF (2017) Stable detonation characteristics of premixed C_2H_4/O_2 gas in narrow gaps. Exp Fluids 58:112